Tagungsband des 15. ÖAGM Arbeitstreffens
in Klagenfurt 24.-26. April 1991

Modelling and New Methods in Image Processing and in Geographical Information Systems

(Modellbildung und neue Methoden in der Bildverarbeitung
und in Geographischen Informationssystemen)

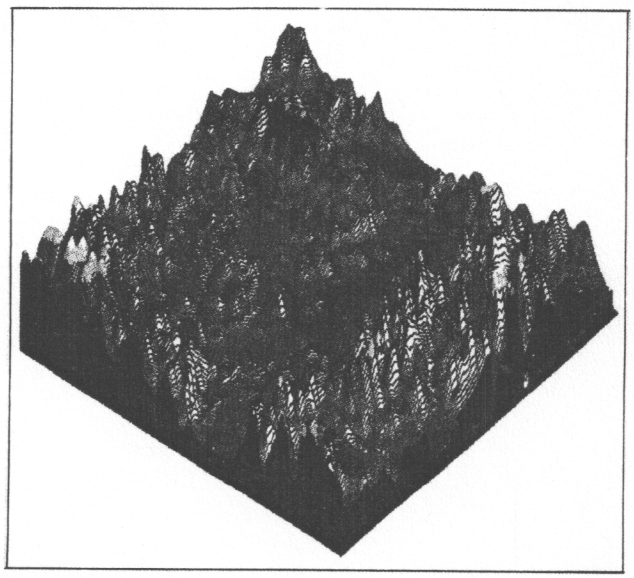

herausgegeben von

Peter Mandl

Österreichische
Computer
Gesellschaft

R. Oldenbourg
Wien
München

CONTENTS

Aleš Jaklič Franc Solina

Computer Vision Laboratory
Faculty of Electrical Engineering and Computer Science
Tržaška 25, 61001 Ljubljana, Slovenia
e-mail: Ales.Jaklic@ninurta.fer.yu

Extracting Reflectance Properties of Materials by Active Vision

ABSTRACT

In this paper we propose a method for detection and separation of diffuse and specular reflection components by using multiple image frames from different viewpoints. The method is based on a hybrid reflectance model and the insight that a specularity is an image of a light source and the image position is dependent on sensor position. Our approach is to move a camera actively and to obtain as many image frames as possible. With known sensor positions, we use a reconstruction algorithm to obtain the object structure as well as the caustic curve according to our geometrical model of diffuse and specular reflection. Experimental results are presented to show the efficiency of our method.

1 Introduction

Most machine vision tasks involve the analysis of intensity images resulting from the interaction of light, scene and sensor. Reflectance properties of materials describe relationships between geometrical, photometrical, spectral, and polarization properties of incident and reflected light in terms of physical laws and models.

Application of these laws and models in machine vision resulted in photometric-stereo type methods to detect specularities and to determine surface orientation by Coleman and Jain [5], and to separate diffuse and specular reflection componenets by Nayar, Ikeuchi and Kanade [8]. Wolff [10] proposed a method using the analysis of polarization of reflected light not only to separate out diffuse and specular components but also to classify the surface type as a dielectric or a metal. Spectral reflectance properties have also been used in color analysis by Klinker, Shafer and Kanade [7], and more recently by Bajcsy, Lee and Leonardis [1] to separate out diffuse and specular components and to detect inter-reflections betwen adjecent objects.

Although all the approaches mentioned above are based on physical models of reflection mechanisms, they have restrictions in applications. The basic technique with the photometric-stereo type approaches is the control of illumination. Therefore the application is limited to the environments where the illumination can be strictly controlled. The polarization approach also has restrictions on sensor and illumination positions. The color approaches are based on two assumptions. One is that object surfaces consist only of colored dielectrics. The other is that the object surface reflectance is spatially piecewise uniform. The second assumption leads to separation of specular and diffuse component by clustering the points of uniform reflectance in color space. The same assumption is required for the polarization approach.

In this paper we propose the use of many images captured from different viewpoints not only to separate the specular from the diffuse component but also to obtain the object structure. Our method is based on the insight that a specularity is an image of a light source and the image position is dependent on sensor position. With active control of sensor position, our algorithm does not require the controlled illumination or the restriction on the material type or on the spatial variation of surface reflectance.

2 Hybrid Reflectance Model

Recently, a hybrid photometric reflectance model was proposed by Nayar [9] composed of three primary components: the diffuse lobe component, the specular lobe component, and the specular spike component. Figure 1 shows a polar plot of image irradiance in case of 2-dimensional geometry.

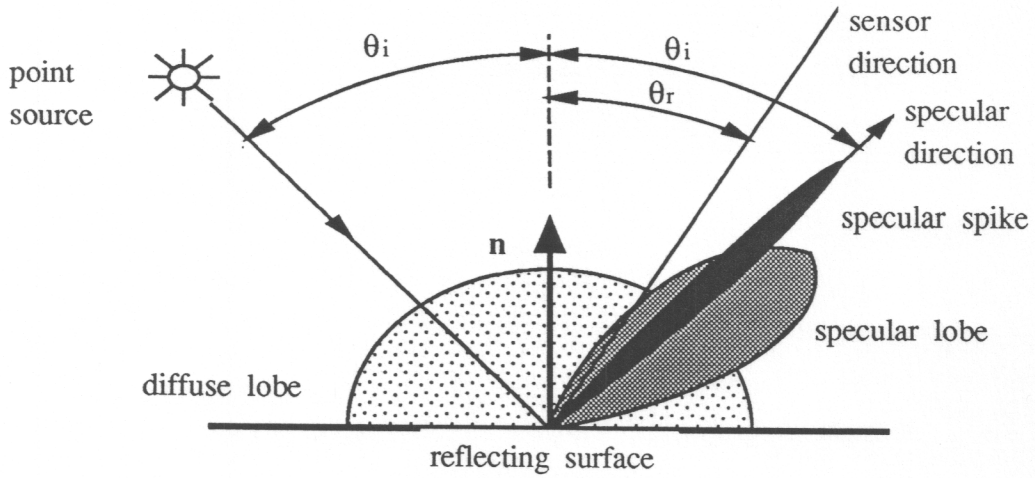

Figure 1: Hybrid reflectance model

The image irradiance as a function of sensor angular position θ_r with respect to surface normal for a fixed source direction can be modelled as a linear combination of all three components

$$I_{im}(\theta_r) = C_{dl} + \frac{C_{sl}}{\cos\theta_r} \exp\left(-\frac{(\theta_i + \theta_r)^2}{8{\sigma_\alpha}^2}\right) + C_{ss}\delta(\theta_i - \theta_r) \tag{1}$$

where the parameter σ_α represents surface roughness and the constants C_{dl}, C_{sl}, and C_{ss} represent the maximal magnitudes of the diffuse lobe component, specular lobe component, and specular spike component, respectively. The magnitude of diffuse lobe component is dependent only on surface irradiance and is modelled by the Lambertian model. On the other hand, image irradiance due to the specular lobe and specular spike component is highly dependent on sensor position and these components are modelled by Torrance-Sparrow model and Beckmann-Spizzichino model, respectively. Note that in general the peak of specular lobe is not in the direction of specular spike—that being in the direction of a perfect specular reflection. To simplify the further analysis we assume that the surfaces are smooth – either the surface roughness parameter σ_α is of the same or lower order as the wavelenght of incident light or the surface is gently

undulating [9]. In either case the specular lobe and spike components have significant magnitude only in a narrow region around the specular direction.

3 Structure Perception in Case of Hybrid Reflectance Model

Smooth surfaces with specular reflection properties form virtual or real images of light sources. Geometrical optics explains why an image is formed behind a smooth convex surface and in general in front of a concave surface. Some experiments with human observers suggest that human visual analysis employs a physical model of specular reflection [4]. In short, a local surface curvature constrains the depth of the image of a light source [2,3]. This constraint can be used to either confirm or reject a hypothesis that we are looking at a specular reflection knowing the approximate surface shape. In case that the specularity does not satisfy the constraint it might be a transparent light source or a specular reflection generated by another transparent surface with only specular reflectance component in front of the opaque surface.

In Figure 2 a specular reflection is illustrated for a 2-dimensional smooth convex surface and a distant point light source.

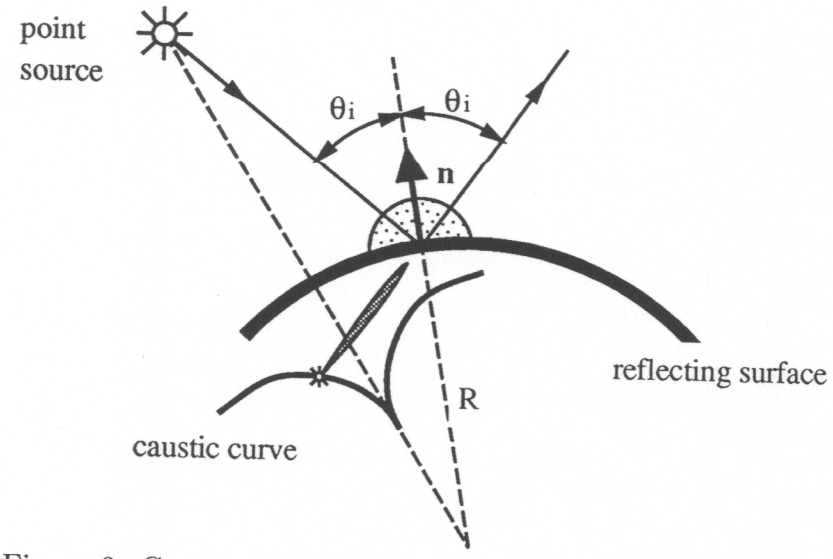

Figure 2: Geometrical model of diffuse and specular reflection

The surface reflects light rays in such a way that the exitant angle equals the incident angle and that the incident and reflected ray lie in a plane containing the surface

normal. The image of point light source is formed at the focus. The focal length is given by (see Appendix A)

$$f = \frac{R}{2} \cos \theta_i \tag{2}$$

where R is the radius of curvature at the point of reflection and θ_i is the incident angle.

As the observer moves the image of a light source at the focus moves too and defines a caustic curve, which is entirely determined by surface shape and position of the light source. Since the image irradiance is the sum of diffuse and specular component, we can model the process of light reflection as a diffuse light source placed on the object surface and a highly collimated light source placed at the focus radiating only in the corresponding direction of specular reflection (Figure 2). Addition of the specular and diffuse component requires that diffuse sources on the surface are transparent for collimated sources located on the caustic curve. On the other hand diffuse sources on the surface are opaque to other diffuse sources because of occlusion.

4 Structure Reconstruction

In search for a method for reconstructing the geometry of our model the following should be considered:

- to observe a change of focus position we need to move our sensor gradually and integrate the information from several image frames and known sensor positions,
- diffuse sources at the surface are transparent for light radiated from collimated sources on the caustic curve.

Although, the image irradiance cannot be directly related to our geometrical model of reflection as an integral projection of spatial radiance distribution of sources because of occlusion among diffuse sources on the surface and apparent movement of the image of the light source, a direct application of a simple filtered backprojection algorithm [6] used in computer tomography has given some interesting results. In Figure 3 camera control scheme is shown. A camera is rotated about a fixed point in the object region

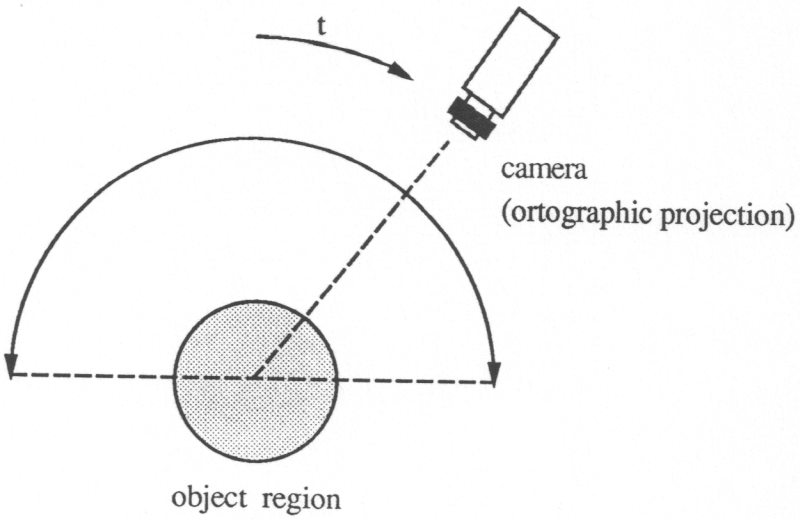

Figure 3: Camera control scheme

and an ortographic projection is assumed.

Figure 4 (a) shows a synthetic input image data for a spherical and Figure 4 (b) for a parabolic surface. On the reconstructed image of the spherical surface in Figure 4 (c) the cusp of the caustic curve also shows the direction of the light source. In some special cases a caustic curve can vanish into a single point. That well known focusing property of parabolic surfaces for a centrally placed light source is illustrated in Figure 4 (d).

An initial experimental result with a real object is presented in Figure 5. Figure 5 (a) shows 4 out of 30 images obtained for 170° of angular span, and Figure 5 (c) and (d) show the collection of data from the 30 different viewpoints for the cross-sectional planes 1 and 2 shown in Figure 5 (b), respectively. The reconstructed surface structures from the 30 images at the cross-sectional planes 1 and 2 is shown in Figure 5 (e) and (f), respectively.

5 Determination of Reflectance Type

Although the reconstructed structures in Figure 5 are indicative of different reflectance types, it is not easy to identify the reflectance type of each point algorithmically. Note

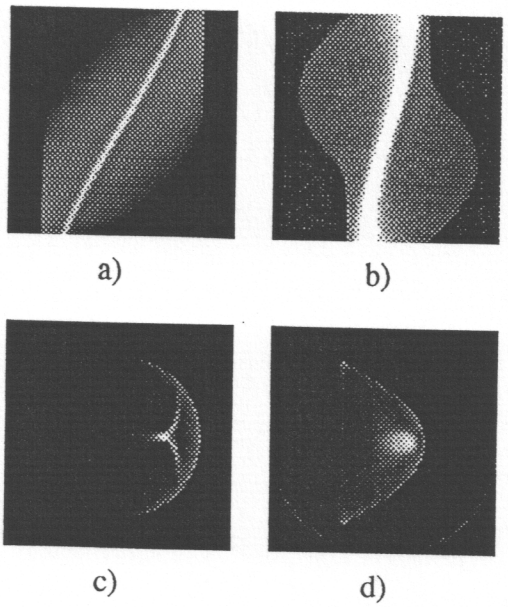

Figure 4: Reconstructed structure (synthetic data)

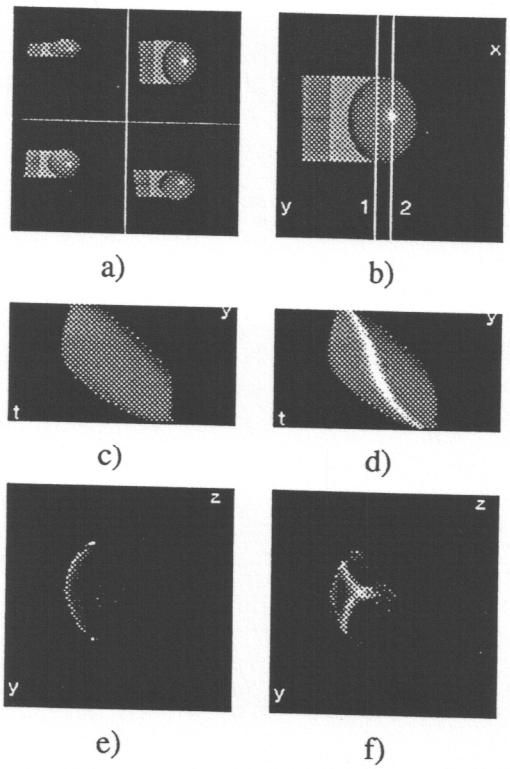

Figure 5: Reconstructed structure (real world data)

that the intensity of the object structure in the reconstructed image is not proportional to the object radiance because the reconstruction method assumes no occlusion. To identify reflectance types systematically we use structure information. If we know the object structure, we can generate a trajectory of a point on the surface in the image sequence and detect if the point is occluded. The next step is to use the image irradiance on the trajectory as a function of sensor position. Figure 6 presents measured image irradiance values for the point on the mouse surface. Image irradiance due to the diffuse component is independent on sensor position and equals the minimum value of the function since the specular component increases the irradiance.

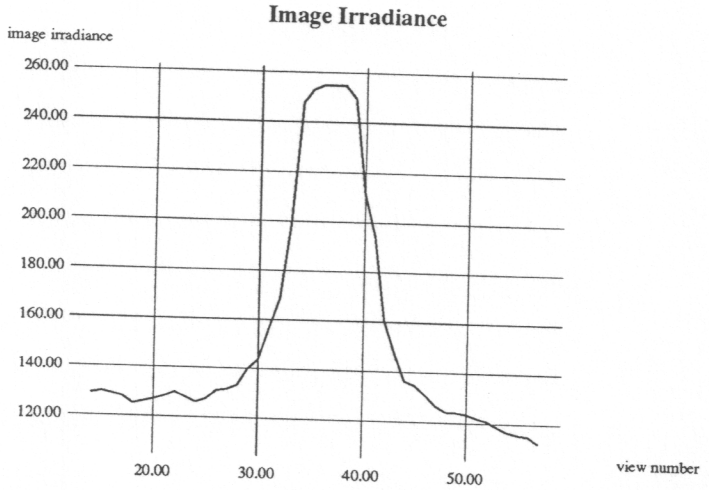

Figure 6: Measured image irradiance at the point on the mouse surface

6 Conclusions and further work

In this paper, we have demonstrated that we can integrate image information captured from different viewpoints to obtain the object stucture and caustic curve according to our geometrical model of diffuse and specular reflection. That allows us to detect and separate diffuse and specular reflectance component.

We think that the presented method could be easilly integrated with color analysis by using a linear reconstruction technique and sets of RGB images. That could led to an approximation of the color of illumination source on the caustic curve.

A Appendix

We would like to find a focus position in the case of 2-dimensional object with smooth boundary represented by $y = f(x), f \in C^2$ and a single distant point light source. The geometry for derivation of the focus position is depicted in Figure 7.

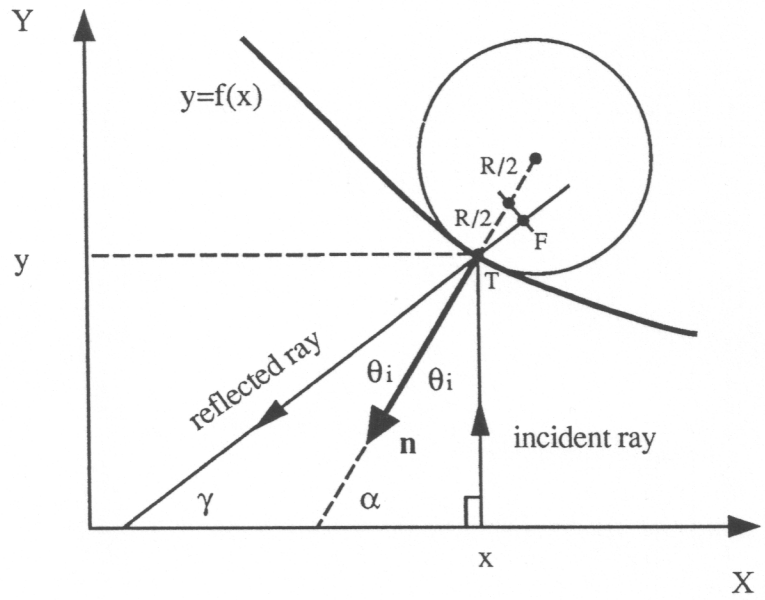

Figure 7: Geometry of specular reflection

Since the source is far away from the surface of the object we can assume that the incident rays are parallel. Without loss of generality we choose the coordinate system such that the rays are parallel to Y axis.

The reflected ray at the point $T = (x, y)$ on curve $y = f(x)$ defines a line

$$-(X - x)\tan\gamma + (Y - y) = 0. \tag{3}$$

Due to the law of reflection angle γ can be expressed as $\gamma = \alpha - \theta_i = 2\alpha - 90°$. Since $\tan\alpha = -\frac{dx}{dy}$ it follows

$$\tan\gamma = \tan(2\alpha - 90°) = -\frac{1 - \left(\frac{dy}{dx}\right)^2}{2\frac{dy}{dx}}. \tag{4}$$

By replacing $\tan\gamma$ in equation (3) by (4) we derive the equation for the reflected ray at the point $T = (x, y)$ on the curve $y = f(x)$

$$(X - x)(1 - \left(\frac{dy}{dx}\right)^2) + 2(Y - y)\frac{dy}{dx} = 0. \tag{5}$$

Note that equation (5) above represents a family of lines, reflected rays $G(X, Y, x) = 0$, with parameter x. We want to find the intersection of two reflected rays which are infinitesimaly "close" with respect to parameter x thus forming a narrow pencil of parallel incident rays. That leads to the system of equations

$$G(X, Y, x) = 0 \qquad \frac{\partial G}{\partial x}(X, Y, x) = 0, \tag{6}$$

that is

$$(X - x)(1 - \left(\frac{dy}{dx}\right)^2) + 2(Y - y)\frac{dy}{dx} = 0 \tag{7}$$

$$-(X - x)\frac{dy}{dx} + (Y - y) = \frac{1 + \left(\frac{dy}{dx}\right)^2}{2\frac{d^2y}{dx^2}}. \tag{8}$$

The equation (8) is the envelope of familly of lines $G(X, Y, x) = 0$. Solving the system for X and Y, we obtain the coordinates of the focus $F = (p, q)$ corresponding to the point $T = (x, y)$, where

$$p = x - \frac{\frac{dy}{dx}}{\frac{d^2y}{dx^2}} \tag{9}$$

$$q = y + \frac{1 - \left(\frac{dy}{dx}\right)^2}{2\frac{d^2y}{dx^2}}. \tag{10}$$

An easy calculation of the distance between points $T = (x, y)$ and $F = (p, q)$ gives

$$\overline{TF} = \frac{1 + \left(\frac{dy}{dx}\right)^2}{2\frac{d^2y}{dx^2}}. \tag{11}$$

Finally, from the radius of curvature R at the point $T = (x, y)$

$$R = \frac{\left[1 + \left(\frac{dy}{dx}\right)^2\right]^{\frac{3}{2}}}{\frac{d^2y}{dx^2}} \tag{12}$$

and

$$\cos\theta_i = \frac{1}{\sqrt{1 + \cot^2\alpha}} = \frac{1}{\sqrt{1 + \left(\frac{dy}{dx}\right)^2}} \tag{13}$$

we derive

$$\overline{TF} = \frac{R}{2}\cos\theta_i. \tag{14}$$

Figure 7 also shows a geometrical construction of the focus position. It is constructed by orthogonal projection of the middle point of curvature radius R in the direction of surface normal onto the line of reflected ray.

References

[1] Ruzena Bajscy, Sang Wook Lee, and Aleš Leonardis. Color image segmentation with detection of highlights and local illumination induced by inter-reflections. In *Proceedings of the 10th International Conference on Pattern Recognition*, 1990.

[2] Andrew Blake. Specular stereo. In *Proceedings of the 9th International Conference on Artificial Intelligence*, pages 973–976, 1985.

[3] Andrew Blake and Gavin Brelstaff. Geometry from specularities. In *Proceedings of the 2nd International Conference on Computer Vision*, pages 394–403, 1988.

[4] Andrew Blake and Heinrich Bülthoff. Does the brain know the physics of specular reflection? *Nature*, 343(11):165–168, January 1990.

[5] E. North Coleman, Jr. and Ramesh Jain. Obtaining 3-dimensional shape of textured and specular surfaces using four-source photometry. *Computer Graphics and Image Processing*, 18(4):309–328, May 1982.

[6] Ashvin C. Kak and Malcom Slaney. *Computerized Tomographic Imaging.* IEEE Press, 1988.

[7] Gudrun J. Klinker, Steven A. Shafer, and Takeo Kanade. The measurement of highlights in color images. *International Journal of Computer Vision*, 2(1):7–32, 1988.

[8] Shree K. Nayar, Katsushi Ikeuchi, and Takeo Kanade. Determining shape and reflectance of hybrid surfaces by photometric sampling. *IEEE Transactions on Robotics and Automation*, 6(4):418–431, August 1990.

[9] Shree K. Nayar, Katsushi Ikeuchi, and Takeo Kanade. Surface reflection: Physical and geometrical perspectives. In *Proceedings of the Image Understanding Workshop*, pages 185–212, 1990.

[10] Lawrence B. Wolff. Using polarization to separate reflection components. In *Proceedings of the IEEE Conference on Computer Vision and Pattern Recognition*, pages 363–369, 1990.